Chinese Journal of Aeronautics, (2014),27(6): 1413–1420

Chinese Society of Aeronautics and Astronautics
& Beihang University

Chinese Journal of Aeronautics

cja@buaa.edu.cn
www.sciencedirect.com

Radical recombination in a hydrocarbon-fueled scramjet nozzle

Zhang Xiaoyuan [a], Qin Lizi [a,*], Chen Hong [b], He Xuzhao [c], Liu Yu [a]

[a] School of Astronautics, Beihang University, Beijing 100191, China
[b] State Key Laboratory of High Temperature Gas Dynamics, Institute of Mechanics, Chinese Academy of Science, Beijing 100190, China
[c] China Aerodynamic Research and Develop Center, Mianyang 621000, China

Received 16 November 2013; revised 29 December 2013; accepted 19 February 2014
Available online 20 October 2014

KEYWORDS

Chemical reactions;
Nozzles;
Performance calculation;
Radical;
Recombination

Abstract To reveal the radical recombination process in the scramjet nozzle flow and study the effects of various factors of the recombination, weighted essentially non-oscillatory (WENO) schemes are applied to solve the decoupled two-dimensional Euler equations with chemical reactions to simulate the hydrocarbon-fueled scramjet nozzle flow. The accuracy of the numerical method is verified with the measurements obtained by a shock tunnel experiment. The overall model length is nearly 0.5 m, with inlet static temperatures ranging from 2000 K to 3000 K, inlet static pressures ranging from 75 kPa to 175 kPa, and inlet Mach numbers of 2.0 ± 0.4 are involved. The fraction Damkohler number is defined as functions of static temperature and pressure to analyze the radical recombination progresses. Preliminary results indicate that the energy releasing process depends on different chemical reaction processes and species group contributions. In hydrocarbon-fueled scramjet nozzle flow, reactions with H have the greatest contribution during the chemical equilibrium shift. The contrast and analysis of the simulation results show that the radical recombination processes influenced by inflow conditions and nozzle scales are consistent with Damkohler numbers and potential dissociation energy release. The increase of inlet static temperature improves both of them, thus making the chemical non-equilibrium effects on the nozzle performance more significant. While the increase of inlet static pressure improves the former one and reduces the latter, it exerts little influence on the chemical non-equilibrium effects.

1. Introduction

The supersonic combustion ramjet (scramjet) engine is the key to air-breathing hypersonic flight. Internationally, the scramjet engine has been widely investigated, and there is continuing interest in its performance.[1] As a main component of the scramjet, the nozzle makes high enthalpy flow fully expand from the combustion chamber and produces most of thrust,

* Corresponding author. Tel.: +86 10 82313789.
E-mail addresses: zhangxiaoyuan@sa.buaa.edu.cn (X. Zhang), qinlizi@126.com (L. Qin).

Peer review under responsibility of Editorial Committee of CJA.

Production and hosting by Elsevier

http://dx.doi.org/10.1016/j.cja.2014.10.007

whose magnitude and direction have decisive effects on the scramjet performance.[2] Thus related research is necessary.

Due to high speed, a thermal and chemical non-equilibrium phenomenon is visible in the external and internal flow fields of a hypersonic vehicle, and different regions require different levels of chemical and thermal modeling.[3] One of the characteristics of the scramjet nozzle flow is the chemical non-equilibrium flow. The scramjet operating temperature is extremely high and a fuel-sufficient combustion is difficult because of the exceedingly high speed. Radical recombination and kinetic afterburning exist in the nozzle flow,[4,5] which causes some chemical energy released during the nozzle flow. Because of this effect, the distributions of the wall pressure get a change and the nozzle performance is improved.

Previous studies on the chemical non-equilibrium nozzle flow mostly focused on calculation methods and effects on nozzle performance, mainly based on a hydrogen-fueled scramjet nozzle. The chemical non-equilibrium process in the nozzle was rarely discussed, especially the radical recombination as its effects on nozzle performance appeared only in high-temperature conditions. A computer model for describing quasi-one-dimensional flow was used by Sangiovanni et al.[6] to study the role of hydrogen/air chemistry in nozzle performance for a hypersonic propulsion system. The study showed that the finite-rate chemistry should not be neglected in nozzle performance simulations, because the beneficial chemical process persisted throughout the entire nozzle length. Thomas and Wolfgang[7] used a finite element code to model the chemical reactions considering the finite-rate chemistry and the vibrational relaxations. Different test cases were computed, and the results were compared with the measured data. Stallker et al.[4] thought that kinetic afterburning could be taken as occurring when the combustion reaction was interrupted by the nozzle expansion. The reactions were not completely quenched and proceeded to produce substantial heat release in the nozzle. Wang's study[8] indicated that the nozzle could supplement the combustion in a supersonic combustor so that the performance of the nozzle could be increased.

The high temperature makes the gas dissociate partially in the scramjet combustion, and the radical components recombine in the nozzle due to the decrease of temperature with some energy released to increase the nozzle performance. This paper aims at analyzing the phenomenon of radical recombination in the nozzle flow and studying the effect on the scramjet nozzle performance, based on a perfect combustion at the exit of a kerosene-fueled scramjet combustor.

2. Numerical simulation and verification

2.1. Physical model

As shown in Fig. 1, the vehicle studied is a fully integrated scramjet[9] which employs the entire windward surface of the forebody in the inlet compression process and the entire windward surface of the afterbody in the exhaust expansion process. A representative entire-cowl two-dimensional nozzle is designed by the cubic spline curve method. The geometric parameters of the nozzle used in experiments and numerical simulations are: nozzle total length $L = 0.497$ m, nozzle entrance height $H_{\text{in}} = 0.047$ m, nozzle exit height $H_{\text{out}} = 0.241$ m, and nozzle width $W = 0.06$ m.

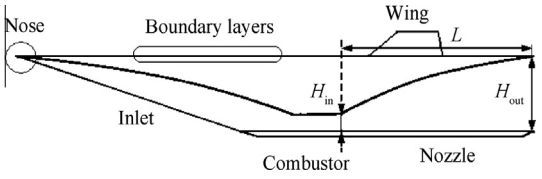

Fig. 1 General configuration of a hypersonic vehicle.

2.2. Numerical method

The scramjet nozzle expansion process is modeled in sufficient details to adequately simulate the pressure/temperature history in the nozzle, and thereby is able to isolate the role of chemical reaction mechanisms. Since the emphasis of this study is on nozzle chemistry, the effects due to viscosity and mixing are neglected in this model. On the basis of the assumptions, the governing equations are made from the two-dimensional Euler equations with the conservation of mass in Cartesian coordinates, applying 17 species and 26 elementary reaction models:

$$\frac{\partial \boldsymbol{U}}{\partial t}+\frac{\partial \boldsymbol{E}}{\partial x}+\frac{\partial \boldsymbol{F}}{\partial y}=\boldsymbol{S} \tag{1}$$

where the conservative vector $\boldsymbol{U}=[\rho,\rho u,\rho v,\rho e,\rho_1,\rho_2,\cdots,\rho_{n-1}]^{\mathrm{T}}$, $\boldsymbol{E}$ and $\boldsymbol{F}$ are convective terms, and $\boldsymbol{S}=[0,0,0,0,\sigma_1,\sigma_2,\cdots,\sigma_{n-1}]^{\mathrm{T}}$ is a source term; ρ is the density; u and v are the velocity components in x-direction and y-direction; e is the specific internal energy; ρ_i and σ_i are the density and mass production rate of each species, and $\sum_{i=1}^{n}\sigma_i=0$, $\sum_{i=1}^{n}\rho_i=\rho$.

The governing equations are decoupled by the method proposed in Refs.[10,11]. Firstly, the equations are mathematically transformed by

$$\rho e^{*}=\rho e-\sum_{i=1}^{n}\rho_i h_i^0(T)=0.5\rho(u^2+v^2)+\frac{p}{\gamma-1} \tag{2}$$

where e^{*} and γ have no precise physical meanings, but they are equivalent to the internal energy and specific heat ratio of perfect gas in mathematical forms; p is the pressure and h_i^0 is the standard state specific enthalpy of species i. The variable e in the conservative vector $\boldsymbol{U}$ is replaced with e^{*}, and the source term gets a new transformation of

$$\boldsymbol{S}^{*}=\left[0,0,0,-\sum_{i=1}^{n}\sigma_i h_i^0(T),\sigma_1,\sigma_2,\cdots,\sigma_{n-1}\right]^{\mathrm{T}} \tag{3}$$

Then, the equations are divided into two parts, flow equations and chemical equations, according to the operator splitting method as follows:

$$\frac{\partial \boldsymbol{U}}{\partial t}+\frac{\partial \boldsymbol{E}}{\partial x}+\frac{\partial \boldsymbol{F}}{\partial y}=\boldsymbol{0} \tag{4}$$

$$\frac{\partial \boldsymbol{U}}{\partial t}=\boldsymbol{S}^{*} \tag{5}$$

To ensure the second-order accuracy of the solution, Strang splitting is used to decouple the equations. While the equivalent of specific heat ratio is introduced, the flow equations are similar to the Euler equations of perfect gas, and upwind WENO schemes[12,13] are applied.

Table 1 17 species and 26 steps kerosene–air reaction mechanism.[14]

No.	Reaction	A	n	E_a	No.	Reaction	A	n	E_a
1	$N_2 + C_{12}H_{23} \Rightarrow 12CH + 11H + N_2$ /N_2 0.8/ $C_{12}H_{23}$ 0.8/	4.35×10^{9}	0	30000	12	$CO + OH = CO_2 + H$	1.51×10^{7}	1.28	−758
					13	$CH + O = CO + H$	3.00×10^{12}	1	6000
2f	$CH + H_2 + N_2 \Rightarrow 2NH + CH$ /CH 1.0/ H_2 0.1/ N_2 1.0/	1.00×10^{15}	0	78000	14	$CH + OH = CO + H2$	3.00×10^{13}	0	0
					15	$CH + NO = NH + CO$	1.00×10^{11}	0	0
2b	$CH + 2NH \Rightarrow N_2 + H_2 + CH$ /CH 1.0/ NH 2.0/	1.95×10^{15}	0	0	16	$N_2 + 2CH = C_2H_2 + N_2$	1.00×10^{14}	0	0
					17	$C_2H_2 + O_2 = 2CO + H_2$	3.00×10^{16}	0	19000
3	$H_2 + OH = H_2O + H$	1.17×10^{11}	1.3	3626	18	$N_2 + O = N + NO$	6.50×10^{13}	0	75000
4	$O + H_2 = OH + H$	2.50×10^{15}	0	6000	19	$N + O_2 = NO + O$	6.30×10^{9}	1	6300
5	$H + O_2 = OH + O$	4.00×10^{14}	0	18000	20	$N + OH = NO + H$	3.00×10^{11}	0	0
6f	$N_2 + O_2 \Rightarrow 2O + N_2$	1.00×10^{18}	0	122239	21	$NH + NO = N_2O + H$	2.00×10^{15}	−0.8	0
6b	$H_2 + 2O \Rightarrow O_2 + H_2$	1.00×10^{18}	0	0	22	$N_2O + OH = N_2 + HO_2$	3.20×10^{13}	0	0
7	$H_2 + 2H = 2H_2$	2.00×10^{17}	0	0	23	$N_2O + O = 2NO$	6.00×10^{14}	0	28200
8	$H + O_2 = HO_2$	1.00×10^{15}	−1.01	0	24	$N_2O + O = N_2 + O_2$	6.00×10^{14}	0	28200
9	$H + HO_2 = H_2 + O_2$	6.50×10^{13}	0	0	25	$N_2O + H = N_2 + OH$	1.50×10^{12}	0	0
10	$O + HO_2 = OH + O_2$	2.50×10^{13}	0	0	26	$NH + O = NO + H$	2.50×10^{4}	2.64	0
11	$CO + HO_2 = CO_2 + OH$	5.80×10^{13}	0	22934					

Note: rate coefficients are in the form of $k = AT^n\exp(-E_a/(RT))$; f represents forward reaction and b represents backward reaction.

2.3. Reaction mechanism

The 17 species and 26 steps kerosene–air chemical reaction models shown in Table 1 are employed to calculate by Arrhenius' equation, where k is the rate constant, T is the absolute temperature, A is the pre-exponential factor, E_a is the activation energy, and R is the universal gas constant. In Kundu's study,[14] the ignition delay times of the models were close to the experiment values and the models were suitable for the calculation of supersonic combustion. Chang and Lewis[15] used the reaction models in the study of scramjet numerical simulation and reasonable results were achieved.

A direct comparison is made between results of calculated and experimental data of ignition delay with the gas parameters close to those in a nozzle. Fig. 2(a) shows the predicted and experimental data of ignition delay obtained by Freeman and Lefebvre[16] versus the reciprocal of the inlet mixture temperature varied from 920 K to 1040 K for an equivalence ratio of 0.5 and a pressure of 0.1013 MPa. Although the predicted ignition is much quicker at lower temperature, the agreement between experiment and prediction is not far-off at higher temperature. Fig. 2(b) shows the comparison of predicted delays and data measured by Mikolaitis et al.[17] in the temperature range of 1200–2000 K and there is a good agreement between the calculated and experimental data. The comparisons verify that the mechanism is applicable to simulate the nozzle flow.

2.4. Experimental verification

A ground experiment was carried out using a shock tunnel[18,19] to verify the feasibility of the numerical results. A double detonation driver[20] was applied to produce high enthalpy gas steadily to simulate the condition of the scramjet nozzle at a high Mach number. As shown in Fig. 3, the equipment is almost the same as a conventional shock tunnel, but the difference is the detonation in the driven section. The detonation gas was obtained with the same temperature, pressure, and components of the scramjet, by controlling the fuel ratio, as well as the pressure and temperature at the end of the detonation tube. The stagnation pressure and stagnation temperature can be acquired accurately in the driven section so that the components of the gas are accessible. The gas is accelerated to a desired speed by the Laval nozzle.

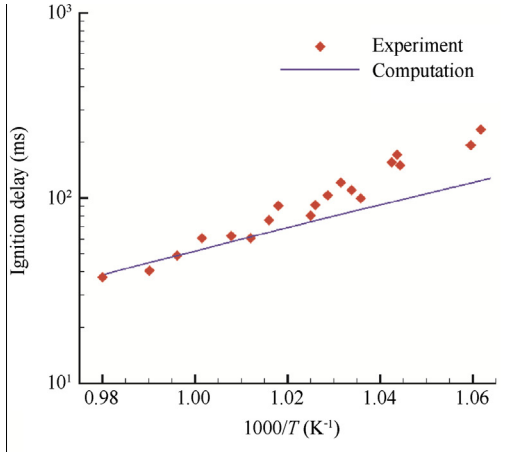

(a) Computational results and experimental data obtained by Freeman and Lefebvre[16]

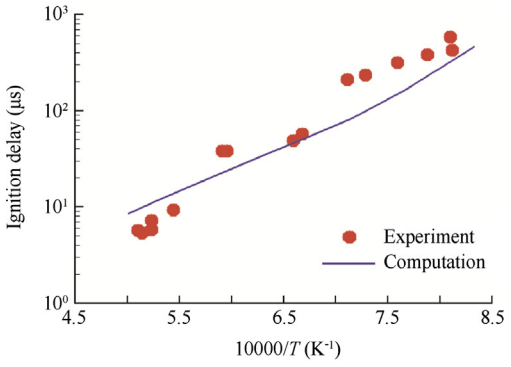

(b) Computational results and experimental data obtained by Mikolaitis et al.[17]

Fig. 2 Comparison of experimental and calculated ignition delay of kerosene.

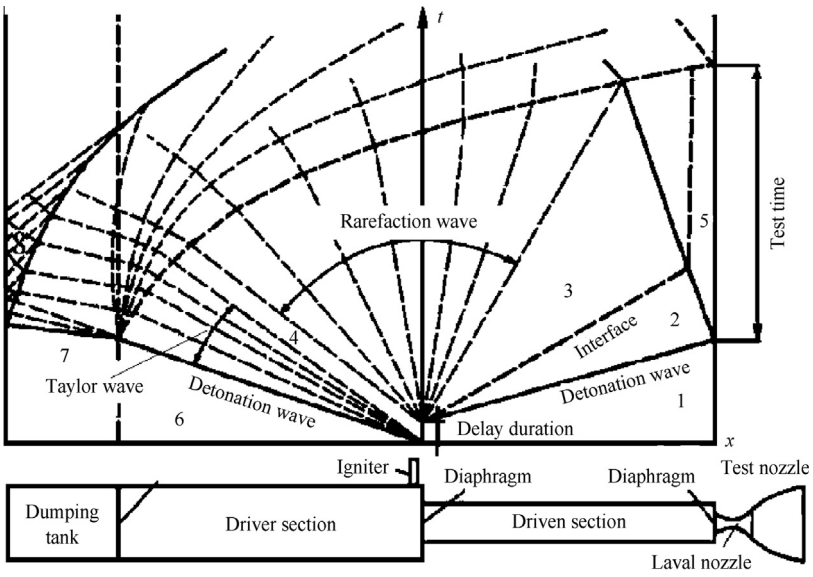

Fig. 3 Principle of producing high enthalpy gas by the double detonation method.

Table 2 Test conditions.

Parameter	Value
Stagnation pressure (kPa)	677
Stagnation temperature (K)	3300
Mass fraction of N_2 (%)	69.31
Mass fraction of O_2 (%)	12.28
Mass fraction of H_2 (%)	9.21
Mass fraction of C_2H_2 (%)	3.07
Mass fraction of CO_2 (%)	6.14

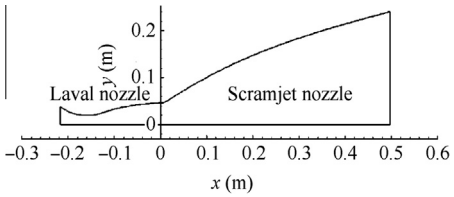

Fig. 4 Calculated field for the test.

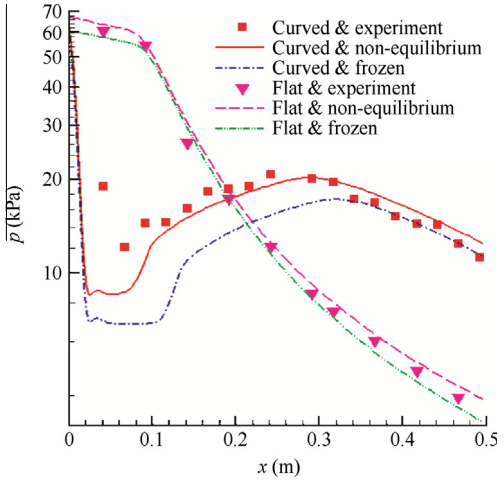

Fig. 5 Pressure distributions on the nozzle wall.

The test conditions shown in Table 2 are the operating parameters of the driven section achieving a Mach number of 2.2 at the test nozzle inlet. The calculated field for the test contains the Laval nozzle and the test nozzle as shown in Fig. 4, and the structured grids are generated after independence check. The mass fractions of the gas in the chemical equilibrium state are calculated by the equilibrium constant method. The adiabatic and slip condition is applied to the solid wall boundary.

In Fig. 5, the pressure distributions on the curved and flat nozzle walls calculated with the chemical frozen or non-equilibrium model are compared with the experimental measurements. As single expansion-ramp nozzle flow is asymmetric, the pressure distributions on the curved and flat walls are totally different. The pressure on the flat wall decreases along the flow direction, while the pressure on the curved wall drops off quickly at the entrance. For this reason, the predicted value of the curved-wall pressure is in poor agreement compared with experimental data near the entrance. The calculated result with the non-equilibrium models is closer to the measured value particularly in the front of the nozzle where a greater contribution to the trust is made. In general, the experimental data make an effective inspection of the numerical method.

3. Analysis of dissociation energy releasing processes

Since the gas rapidly expands in the nozzle, the chemical equilibrium being assumed at the exit of the combustor cannot be maintained. The radical components recombine along with the expanded flow and the dissociation energy release in this way. The equilibrium shift is estimated to analyze the chemical non-equilibrium processes in the nozzle. The parameters at the nozzle exit can be calculated approximately by the one-dimensional theory of steady compressible fluid flow with the entrance parameters known.

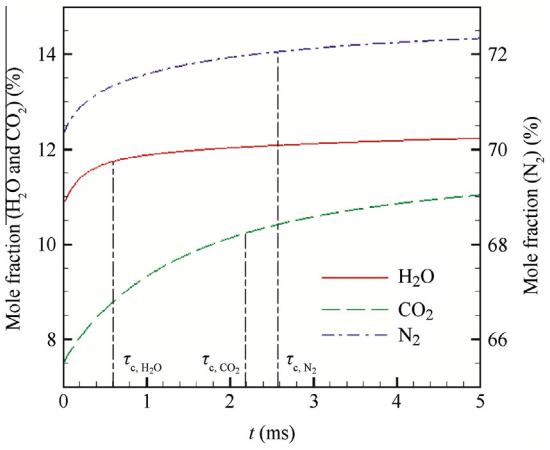

Fig. 6 Fractions-time variations in the chemical equilibrium shift.

The equilibrium shift is calculated with the initial pressure and temperature at the nozzle exit, and the initial values of the fractions are the values at the entrance. Fig. 6 shows the fractions-time variation curves under the condition with an inlet of $Ma = 2.2$, $T = 2700$ K, and $p = 100$ kPa. The variations of H_2O, CO_2, and N_2 have been given in Fig. 6, and they reflect the chemical reaction progresses containing elements of H, C, and N, respectively. At time $t = 0$ ms, the gas in chemical equilibrium at the entrance cannot stay at the equilibrium state under conditions of exit. The fractions of H_2O, CO_2, and N_2 start to increase due to the chemical equilibrium shift and the increasing rates gradually slow down as the Fig. 6 shows. The fraction of H_2O reaches the equilibrium value much earlier, which means that the chemical reactions containing H progress more quickly.

The chemical time scale of one component $\tau_{c,i}$ is the time when the component reaches 50% of the shift process, which is defined as follows:

$$x_i^{\tau_{c,i},\text{out}} = x_i^{\text{in}} + 50\%(x_i^{\text{eq,out}} - x_i^{\text{in}}) \tag{6}$$

where x_i is the fraction of species i, superscript "in" and "out" represent nozzle entrance and exit, and superscript "eq" represents chemical equilibrium. Namely, the change of the component fraction reaches 50% of the change of the chemical shift at that time. The τ_c values of H_2O, CO_2, and N_2 are marked in Fig. 6. As shown in Fig. 6, τ_{c,H_2O} is much smaller and that explains that hydrogen chemical reaction is much faster than the others.

The Damkohler number is defined in a chemical non-equilibrium process at very high velocities of the fluid and the chemical reaction flow is divided into three models, i.e., the chemical frozen, equilibrium, and non-equilibrium models. In the scramjet nozzle flow, the influence of convective terms in the governing equations is much more significant than that of diffusive terms, so the first Damkohler number is accepted and corresponds to the ratio of the flow time scale τ_f to the chemical time scale τ_c as follows:

$$D_I = \frac{\tau_f}{\tau_c} \tag{7}$$

If $D_I \to \infty$, there is enough time to complete the chemical reaction during the flow process and it is chemical equilibrium flow. When $D_I \to 0$, the residence time in the flow field is short for the chemical reaction and it is chemical frozen flow. When D_I is close to 1, τ_f and τ_c are in the same order of magnitude and the flow is chemical non-equilibrium.

The flow time scale τ_f is defined as follows:

$$\tau_f = L/\bar{v} = \frac{L}{(v^{\text{in}} + v^{\text{out}})/2} \tag{8}$$

where $\bar{v}$ is the average velocity; v^{in} and v^{out} are the velocity of nozzle entrance and exit.

Fig. 7 shows the variations of D_I numbers with T and p of the nozzle inlet when the nozzle inlet Mach is 2.2. Three kinds of D_I numbers including H_2O, CO_2, and N_2 are given to compare the different chemical reaction processes containing H, C, or N. All the D_I numbers increase quickly as the inlet temperature increases as Fig. 7(a) shows. The values are of the same order of magnitude with 10^{-3} when the inlet temperature is 2000 K, while they increase to the order of magnitude of 10^{-1} when the inlet temperature is 3000 K. That means the chemical reaction is frozen when the inlet temperature is 2000 K, while it cannot be neglected when the inlet temperature is 3000 K by the definition of D_I numbers. The D_I numbers increase with the inlet pressure increasing as shown in Fig. 7(b), but the relative growth of D_I numbers caused by pressure is not as big as that caused by temperature.

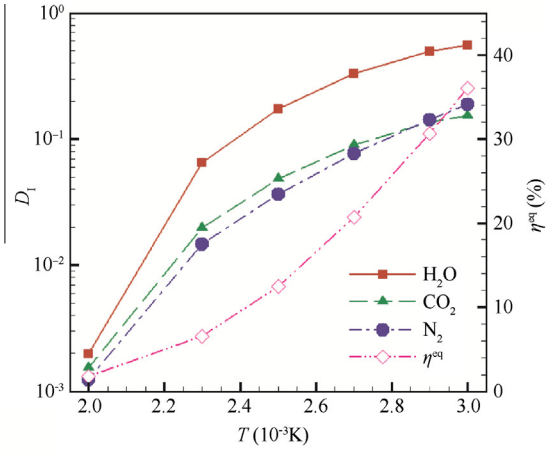

(a) T=2000-3000 K, p=100 kPa

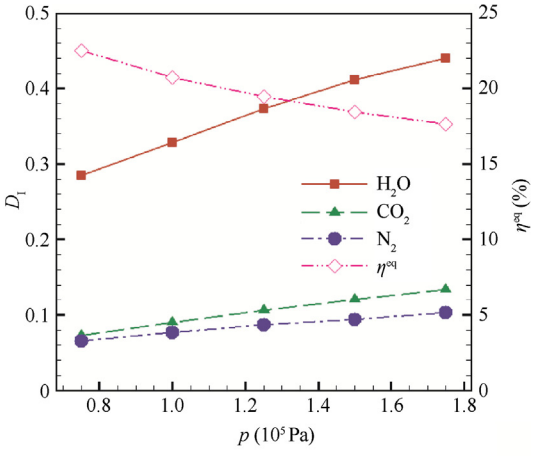

(b) p=75-175 kPa, T=2700 K

Fig. 7 Variations of D_I and η^{eq} with T and p ($Ma = 2.2$).

In all conditions calculated, D_{l,H_2O} is one order of magnitude larger than D_{l,CO_2} and D_{l,N_2}. That indicates the chemical reaction process containing hydrogen requires less time, and the process is faster than the others in the nozzle flow.

The amount of energy released from radical recombination is the most when reaching chemical equilibrium at the nozzle exit. The definition of η^{eq} is the ratio of the decrease of the specific enthalpy when reaching chemical equilibrium to the specific kinetic energy of the inlet as follows:

$$\eta^{eq} = \frac{\Delta h}{0.5v^2} = \frac{\sum_{i=1}^{n} x_i^{in} h_i(T^{out}) - \sum_{i=1}^{n} x_i^{out,eq} h_i(T^{out})}{0.5v^2} \tag{9}$$

where η^{eq} indicates the relative amount of the most energy that can be released during the flow. Fig. 7 also shows the variation of η^{eq} with the inlet static temperature and pressure. The value of η^{eq} increases rapidly with the increase of the temperature, while it decreases with the increase of the pressure. That is because higher temperature promotes dissociation while higher pressure inhibits it. The increase of the inlet temperature not only accelerates the recombination, but also increases the potential energy. Therefore, it should enhance the effect of chemical non-equilibrium significantly.

The chemical reaction processes containing H, C, or N have different reaction rates as previously stated, which have different contributions to the energy released. All the species are divided into four groups: H group (H, H_2O, OH, H_2, and HO_2), C group (CO, CO_2, CH, and C_2H_2), N group (N, NO, N_2O, N_2, and NH), and O group (O and O_2). Fig. 8 shows the variations of the energy contribution ratios of each group with the inlet static temperature. H group and C group are major contributors, and the ratio of H group increases with increasing temperature. The contribution ratio of N group always approximates 5%, so the reactions containing N have less chemical energy released.

4. Influences of various factors on radical recombination

The chemical non-equilibrium effect on the nozzle is caused by radical recombination in the case of complete combustion at the inlet. δ is defined to quantify the chemical non-equilibrium effect on nozzle performance and it is the relative increment of the nozzle thrust values calculated with the chemical non-equilibrium model to those with the frozen model as follows:

$$\delta = \frac{F_x^{Ch} - F_x^{Fr}}{F_x^{Fr}} \tag{10}$$

where F_x is the nozzle thrust, superscripts "Ch" and "Fr" represent chemical non-equilibrium model and chemical frozen model. Use the numerical methods described previously to simulate the nozzle flow with the chemical non-equilibrium and frozen models and get the nozzle thrust value by integrations of the wall pressure. Fig. 9 presents the calculation results of the pressure contour in chemical non-equilibrium flow.

Eq. (11) gives the definition of η, which is the ratio of the decrease of the specific enthalpy between the inlet and the outlet to the specific kinetic energy of the inlet. This is quantification of the chemical energy released during the nozzle flow. ε_i is defined the same as in Eq. (12) to describe the progress of the chemical equilibrium shift to species i. Species i is closer to equilibrium, when ε_i is closer to 100%.

$$\eta = \frac{\Delta h}{0.5v^2} = \frac{\sum_{i=1}^{n} x_i^{in} h_i(T^{out}) - \sum_{i=1}^{n} x_i^{out} h_i(T^{out})}{0.5v^2} \tag{11}$$

$$\varepsilon_i = \frac{x_i^{out} - x_i^{in}}{x_i^{eq} - x_i^{in}} \tag{12}$$

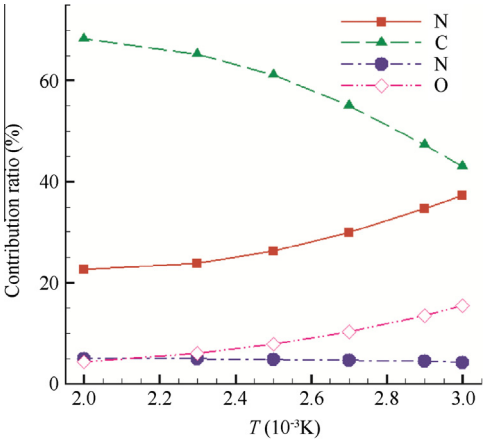

Fig. 8 Variations of the energy contribution ratios with the inlet static temperature (Ma = 2.2, p = 100 kPa).

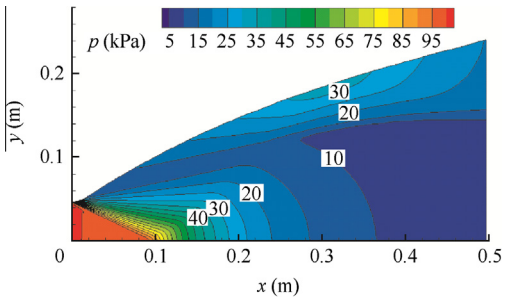

Fig. 9 Pressure contour (Ma = 2.2, p = 100 kPa, T = 2700 K).

4.1. Influences of inlet static temperature and pressure

Fig. 10 demonstrates the variations of δ, η, and ε_i with static temperature and pressure of the nozzle inlet. When Ma = 2.2 and p = 100 kPa, δ increases from less than 0.03% to nearly 5% with the increase in static temperature from 2000 K to 3000 K as shown in Fig. 10(a). Thus the chemical non-equilibrium effects on nozzle performance cannot be neglected at higher temperature. Simultaneously η increases in lockstep with δ, while ε_i has a gentle increase relatively. That reflects the chemical non-equilibrium effects are closely related to the chemical energy released during the nozzle flow. ε_{H_2O} increases from 13.4% to 22.8%, while ε_{CO_2} and ε_{N_2} increase from 1%–2% to nearly 15%. The acceleration of recombination progress is one reason to explain the increase of chemical energy released with the temperature increasing, and the other one is the increase of potential dissociation energy as previously noted. Both of them result in more significant chemical non-equilibrium effects.

When Ma = 2.2 and T = 2700 K, ε_i increases with the inlet static pressure increasing from 75 kPa to 175 kPa as Fig. 10(b) shows, but δ and η remain unchanged essentially, because the

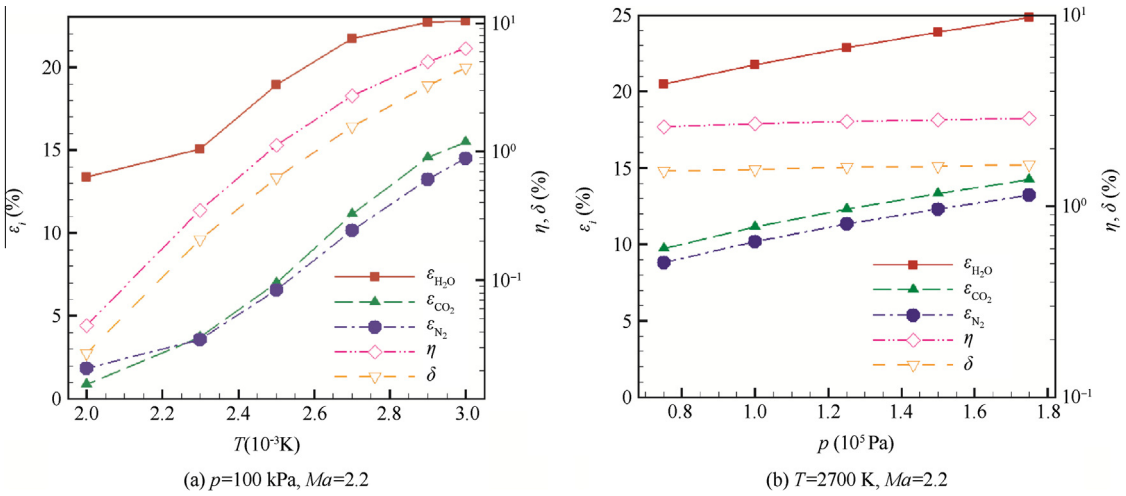

(a) p=100 kPa, Ma=2.2 (b) T=2700 K, Ma=2.2

Fig. 10 Variations of δ, η, and ε_i with the inlet static temperature and pressure.

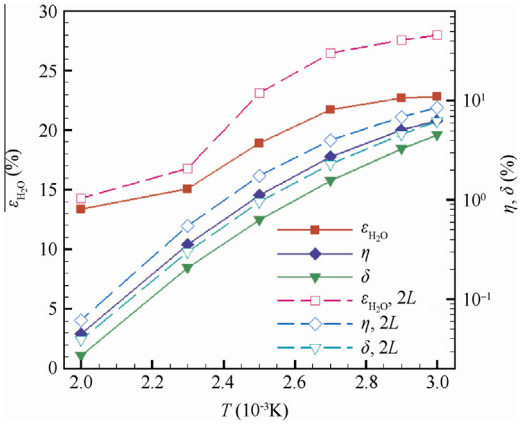

Fig. 11 Variations of δ, η, and ε_{H_2O} with the inlet static temperature (p = 100 kPa, Ma = 2.2).

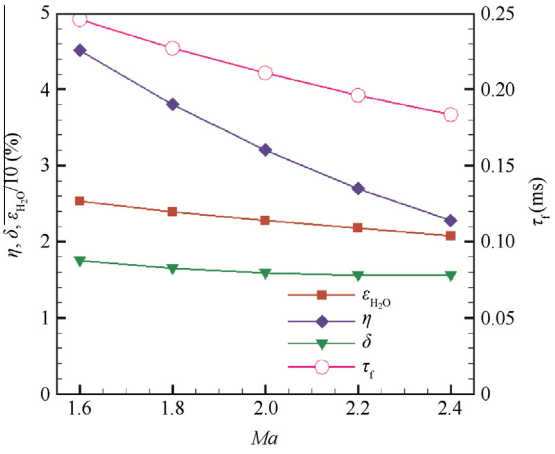

Fig. 12 Variations of δ, η, τ_f, and ε_{H_2O} with the inlet Mach (T = 2700 K, p = 100 kPa).

potential dissociation energy decreases with the increase of the pressure. Therefore, the inlet pressure has little influence on the chemical non-equilibrium effects on nozzle performance.

4.2. Influence of nozzle scales

Another nozzle model with a 2L length obtained by doubling the scale of the original one is used to analyze the influence of nozzle scale on radical recombination. As the inlet static temperature has significant influences and the chemical reaction process containing hydrogen is faster, Fig. 11 gives variations of δ, η, and ε_{H_2O} with the inlet static temperature. The variations of δ, η, and ε_{H_2O} for the 2L nozzle are the same as those for the L nozzle, but the values are always higher. With the increase of the nozzle scale, τ_f and D_I numbers increase. Therefore, the chemical reactions progresses get better at the nozzle outlet and the chemical non-equilibrium effects on nozzle performance are more significant.

4.3. Influence of inlet Mach

With the increase of the nozzle inlet Mach, τ_f and D_I numbers decrease, so the chemical reactions have less time. As Fig. 12 shows, the variations with the inlet Mach from 1.6 to 2.4, ε_{H_2O} and η both decrease with increasing inlet Mach, which means that the chemical reactions progresses get worse. Therefore, the chemical non-equilibrium effects on nozzle performance are weakened.

5. Conclusions

(1) Radical recombination is one reason that makes the scramjet nozzle flow chemical non-equilibrium and affects the nozzle performance. The relative impact of chemical non-equilibrium on nozzle performance exceeds 1% which cannot be neglected when the inlet static temperature reaches 2500 K in this paper.

(2) Reactions with H are much faster in the chemical equilibrium shift in a hydrocarbon-fueled scramjet nozzle. The D_I of H_2O is generally several times larger than those of CO_2 and N_2. Reactions with N have the least potential chemical energy, which is less than 5% of total normally.

(3) The increase of the inlet static temperature not only improves the chemical reaction progresses, but also increases the potential dissociation energy which can be released. δ, used to quantify the effect on the nozzle performance, increases from less than 0.03% to nearly 5% with the temperature from 2000 K to 3000 K according to calculated results.

(4) The increase of the inlet static pressure can accelerate the chemical reactions but reduce the fraction of radical components, so the two opposite effects make the non-equilibrium effect on the nozzle performance change slightly with the pressure.

(5) There is more adequate chemical reaction time due to the increase of the nozzle scale, so the radical recombination progress is improved. While there is less time due to the increase of the nozzle inlet Mach, the effect on nozzle performance is weakened.

References

1. Curran ET. Scramjet engines: the first forty years. *J Propul Power* 2001;**17**(6):1138–48.
2. Li JP, Song WY, Xing Y, Luo FT. Influences of geometric parameters upon nozzle performances in scramjets. *Chin J Aeronaut* 2008;**21**(6):506–11.
3. Bussing TRA, Eberhardt S. Chemistry associated with hypersonic vehicles. *J Thermophys* 1989;**3**(3):245–53.
4. Stallker RJ, Truong NK, Morgan RG, Paull A. Effects of hydrogen-air non-equilibrium chemistry on the performance of a model scramjet thrust nozzle. *Aeronaut J* 2004;**1089**(108):575–84.
5. Zhang XY, Qin LZ, Liu Y. Non-uniform entrance and non-equilibrium chemical effects on scramjet nozzle performance. *J Propul Technol* 2014;**35**(2):166–71 [Chinese].
6. Sangiovanni JJ, Barber TJ, Syed SA. Role of hydrogen/air chemistry in nozzle performance for a hypersonic propulsion system. *J Propul Power* 1993;**9**(1):134–8.
7. Thomas L, Wolfgang WK. Computation of a nonequilibrium expansion flow in a single expansion ramp nozzle. *J Propul Power* 2001;**17**(6):1353–60.
8. Wang XY, Xie GN, Sunden B. Analysis and calculation of chemical non-equilibrium turbulent flow in a scramjet nozzle. *Proceedings of the ASME Turbo Expo* 2009*: power for land, sea, and air*; 2009 Jun 8–12; Orlando, Florida, USA. New York: ASME; 2009. p. 91–6.
9. Joseph MH, James SM, Richard CM. The X-51 scramjet engine flight demonstration program. *Proceedings of 15th AIAA international space planes and hypersonic systems and technologies conference*; 2008 Apr 28–May 1; Dayton, Ohio. Reston: AIAA; 2008.
10. Liu J, Zhang HX, Gao SC. A new uncoupled method for numerical simulation of nonequilibrium flow. *J Natl Univ Defense Technol* 2000;**22**(5):19–23 [Chinese].
11. Liu J. A new nonequilibrium numerical method and simulation of oscillating shock-induced combustion. *Acta Aerodyn Sin* 2003;**21**(1):53–8 [Chinese].
12. Jiang GS, Shu CW. Efficient implementation of weighted ENO schemes. *J Comput Phys* 1996;**126**(1):202–28.
13. Shi J, Zhang YT, Shu CW. Resolution of high order WENO for complicated flow structures. *J Comput Phys* 2003;**186**(2):690–6.
14. Kundu KP, Penko PF, Yang SL. Reduced reaction mechanisms for numerical calculations in combustion of hydrocarbon fuels. *Proceedings of 36th aerospace sciences meeting & exhibit*; 1998 Jan 12–15; Reno, NV. Reston: AIAA; 1998.
15. Chang JS, Lewis MJ. Development of a jet-A/ silane/ hydrogen reaction mechanism for modeling a scramjet combustor. *Proceedings of 35th AIAA/ASME/SAE/ASEE joint propulsion conference and exhibit*; 1999 Jun 20–24; Los Angeles, CA. Reston: AIAA; 1999.
16. Freeman G, Lefebvre AH. Spontaneous ignition characteristics of gaseous hydrocarbon–air mixtures. *Combust Flame* 1984;**58**(2):153–62.
17. Mikolaitis DW, Segal C, Chandy A. Ignition delay for jet propellant 10/air and jet propellant 10/high-energy density fuel/air mixtures. *J Propul Power* 2003;**19**(4):601–6.
18. Yu HR. Oxyhydrogen combustion and detonation driven shock tube. *Acta Mech Sin* 1999;**15**(2):97–107.
19. Li J, Chen H, Yu H. A chemical shock tube driven by detonation. *Shock Waves* 2012;**22**(4):351–62.
20. Chen H, Feng H, Yu HR. Double detonation drivers for a shock tube/tunnel. *Sci China Ser G* 2004;**47**(4):502–12.

Zhang Xiaoyuan is a Ph.D. student in the School of Astronautics at Beihang University. His areas of research include scramjet nozzle experiment and chemical reaction flow.

Qin Lizi is an associate professor in the School of Astronautics at Beihang University. His main research interests include the aerospike nozzle technology, scramjet nozzle and pulse thruster.